Available online at www.sciencedirect.com
ScienceDirect
International Journal of Thermal Sciences 46 (2007) 926–935
International Journal of Thermal Sciences
www.elsevier.com/locate/ijts

Radiation effect on mixed convection laminar flow along a vertical wavy surface

M. Mamun Molla [a], M. Anwar Hossain [b,*,1]

[a] *Department of Mechanical Engineering, University of Glasgow, Glasgow G12 8QQ, UK*
[b] *Department of Mathematics, COMSATS Institute of Information & Technology, Islamabad, Pakistan*

Received 24 July 2006; received in revised form 9 October 2006; accepted 19 October 2006

Available online 4 December 2006

Abstract

The effect of thermal radiation on a steady two-dimensional mixed convection laminar flow of viscous incompressible optically thick fluid along a vertical wavy surface has been investigated. We consider the boundary layer regime when the Reynolds number Re is large. Using the appropriate variables; the basic equations are transformed to convenient form, and then solved numerically employing two efficient method, namely (i) Keller box method (KBM) and (ii) straightforward finite difference (SFFD) method. Numerical results are presented by streamline and isotherms, velocity and temperature distribution of the fluid as well as the, shearing stress, local, average and total heat transfer rate in terms of the skin-friction coefficient, local, average and total Nusselt number respectively for a wide range of the radiation–conduction parameter or Planck number R_d, surface heating parameter θ_w, amplitude of the wavy surface α and the Richardson number $Ri(= Gr/Re^2)$.

Keywords: Radiation effect; Mixed convection; Laminar flow; Vertical wavy surface

1. Introduction

Roughened surfaces are encountered in several heat transfer devices such as flat plate solar collectors and flat plate condensers in refrigerators. Larger scale surface non-uniformities are encountered, for example, in cavity wall insulating systems and grain storage containers. The only papers to date that study the effects of such non-uniformities on the vertical convective boundary layer flow of a Newtonian fluid are those of Yao [1,2], and Moulic and Yao [3,4]. Hossain and Pop [5] have also investigated the magneto-hydrodynamic boundary layer flow and heat transfer from a continuous moving wavy surface, while the problem of free convection flow from a wavy vertical surface in presence of a transverse magnetic field was studied by Alam et al. [6]. Natural convection over a vertical wavy frustum of a cone has been studied by Pop and Na [7]. Cheng and Wang [8] investigated the forced convection in micropolar fluid over a wavy surface. Hossain and Rees [9] have investigated the combined effect of thermal and mass diffusion on the natural convection flow of a viscous incompressible fluid along a vertical wavy surface. The effect of waviness of the surface on the heat and mass flux is investigated in combination with the species concentration for a fluid having Prandtl number equal to 0.7. Hossain et al. [10,11] have studied the problem of natural convection flow along a vertical wavy surface and wavy cone with uniform surface temperature and surface heat flux in presence of temperature dependent viscosity. Molla et al. [12] have investigated the natural convection flow along a vertical wavy surface with heat generation. Jang et al. [13,14] investigated the natural and mixed convection along a vertical wavy surface. Transient analysis of heat and mass transfer by natural convection over a vertical wavy surface has been studied by Jang and Yan [15].

A medium is said to be optically thick if the radiation photon mean free path is very small compared with the characteristic dimension of the medium. This approximation, which is known as the Rosseland or the diffusion approximation, was derived by Rosseland [16]. At high temperatures the presence of thermal radiation alters the distribution of temperature in the

* Corresponding author.
E-mail addresses: cfd@bdcom.com, m.molla@mech.gal.ac.uk (M.M. Molla), anwar@univdhaka.edu (M.A. Hossain).
[1] On leave of absence from the Department of Mathematics, University of Dhaka, Dhaka 1000, Bangladesh.

1290-0729/$ – see front matter
doi:10.1016/j.ijthermalsci.2006.10.010

Nomenclature

$\hat{a}$	dimensional amplitude of the wavy surface
f	dimensionless stream function
g	acceleration due to gravity
Gr	Grashof number
k	thermal conductivity
Nu	Nusselt number
Pr	Prandtl number
q_r	radiation heat flux
q_w	heat flux at the surface
Re	Reynolds number
R_d	radiation–conduction parameter
Ri	Richardson number
T	temperature of the fluid in the boundary layer
T_∞	temperature of the ambient fluid
T_w	temperature at the surface
U_w	inviscid flow solution
u, v	the dimensionless x- and y-component of the velocity
$\hat{u}, \hat{v}$	the dimensional $\hat{x}$ and $\hat{y}$ component of the velocity
x, y	axis in the direction along and normal to the tangent of the surface

Greek symbols

α	dimensionless amplitude of the wavy surface
β	volumetric coefficient of thermal expansion
ψ	stream function
α	amplitude-wavelength ratio
η	non-dimensional similarity variable
ρ	density of the fluid
ν	reference kinematic viscosity
μ	viscosity of the fluid
θ	dimensionless temperature function
θ_w	surface heating parameter
$\sigma(x)$	surface profile function defined in (1)
σ^*	Stefan–Boltzmann constant
α_r	Rosseland mean extinction coefficient
σ_s	scattering coefficient

Subscript

w	wall conditions
∞	ambient temperature
x	differentiation with respect to x

Superscript

$'$	Differentiation with respect to η

boundary layer, which in turn the affects the heat transfer at the wall. In such the situation the simultaneous treatment of the convective and radiative heat transfer is necessary. Goulard and Goulard [17] were among the investigators who studied the coupling between convective and radiative heat transfer for one-dimensional Couette flow. A general treatment of heat transfer by combined convection and radiation in boundary layer flow of a participating fluid leads to a set of partial differential equations, which must be solved simultaneously. The mathematical difficulties involved in handling the resulting system of non-linear partial equations have prompted various investigators to seek approximate method of solving the radiation part of the problem. Several investigators had used the optically thick limit approximation. One of them, Cess [18] studied the interaction of thermal radiation with free convection heat transfer along a vertical flat plate by considering absorbing, emitting and non-scattering gas. He used the singular perturbation technique to solve the set of non-linear partial differential equations. An analytical attempt had been made by Arpaci [19] to understand the non-equilibrium interaction between thermal radiation and laminar free convection from a heated vertical plate immersed in a radiating gas by considering Prandtl number $Pr = 1.0$. Cheng and Ozisic [20] investigated the problem simultaneous radiation and free convection from a vertical plate, considering absorbing, emitting, isotropically scattering fluid. A viscous, radiating, non-similar boundary layer flows from a stagnation region and a flat plate had been investigated by Shwartz [21]. He studied the behavior for an emitting and absorbing gas including the entire range of optical thickness, from thin to thick. Following Cess [18], Hossain et al. [22–24] have analyzed the effect of radiation using Rosseland diffusion approximation which leads to non-similarity solution for the forced and free convection flow of an optically dense viscous incompressible fluid past a heated vertical plate with uniform free stream velocity and surface temperature. Using a group of transformations, the boundary layer equations governing the flow were reduced to local non-similarity equations validating both in the forced and free convection regimes. Radiation effect on free convection along an isothermal vertical cylinder, elliptic cylinder and mixed convection from a horizontal circular cylinder has been investigated by Hossain et al. [25–27]. Yih [28] studied the effect of radiation on natural convection about a truncated cone. Very recently Molla et al. [29] have investigated the radiation effect on natural convection flow from a sphere. To our best of knowledge, radiation effect on mixed convection flow along a vertical wavy surface has not been studied yet and also for considering the practical importance of flat plate solar collector and heat radiator of the home and industry, the present work demonstrates the issue.

Here we have investigated the mixed convection boundary layer flow of an optically dense and viscous incompressible fluid past a vertical wavy surface with effect of thermal radiation using Rosseland diffusion approximation. The boundary layer equations are solved by using Keller box method (KBM) (Cebeci and Bradshaw [30] and Keller [31]) and straightforward finite difference (SFFD) method as Yao [1,2]. We give our attention to the situation where the buoyancy forces assist the flow for various values of the radiation–conduction para-

meter or Planck number R_d, the surface heating parameter θ_w and mixed convection parameter or the Richardson number Ri with Prandtl number $Pr = 1.0$. From these results we can observe the different flow and heat transfer characteristics, which are obtained by varying the relevant parameters.

2. Formulation of the problem

The boundary layer analysis outlined below allows the shape of the wavy surface, $\hat{\sigma}(\hat{x})$, to be arbitrary, but our detailed numerical work will assume that the surface exhibits sinusoidal deformations. Thus the wavy surface is described by

$$\hat{y}_w = \hat{\sigma}(\hat{x}) = \hat{a}\sin^2\left(\frac{\pi\hat{x}}{L}\right) \tag{1}$$

where L is half of the wavelength of the wavy surface, $\hat{a}$ is the amplitude of the waviness. The geometry of the wavy surface and the two-dimensional Cartesian coordinate system are as shown in Fig. 1.

We consider the flow to be governed by the following equations:

$$\frac{\partial\hat{u}}{\partial\hat{x}} + \frac{\partial\hat{v}}{\partial\hat{y}} = 0 \tag{2}$$

$$\hat{u}\frac{\partial\hat{u}}{\partial\hat{x}} + \hat{v}\frac{\partial\hat{u}}{\partial\hat{y}} = -\frac{1}{\rho}\frac{\partial\hat{p}}{\partial\hat{x}} + \frac{\mu}{\rho}\nabla^2\hat{u} + g\beta(T - T_\infty) \tag{3}$$

$$\hat{u}\frac{\partial\hat{v}}{\partial\hat{x}} + \hat{v}\frac{\partial\hat{v}}{\partial\hat{y}} = -\frac{1}{\rho}\frac{\partial\hat{p}}{\partial\hat{y}} + \frac{\mu}{\rho}\nabla^2\hat{v} \tag{4}$$

$$\hat{u}\frac{\partial T}{\partial\hat{x}} + \hat{v}\frac{\partial T}{\partial\hat{y}} = \frac{k}{\rho C_p}\nabla^2 T - \frac{1}{\rho C_p}\nabla\cdot q_r \tag{5}$$

where $(\hat{x}, \hat{y})$ are the dimensional coordinates in the vertical and horizontal directions, $(\hat{u}, \hat{v})$ are the velocity components parallel to $(\hat{x}, \hat{y})$, g is the acceleration due to gravity, $\hat{p}$ is the pressure of the fluid, ρ is the density, ν is the kinematic viscosity, μ is the viscosity of the fluid, k is the thermal conductivity of the fluid and C_p is the specific heat at constant pressure.

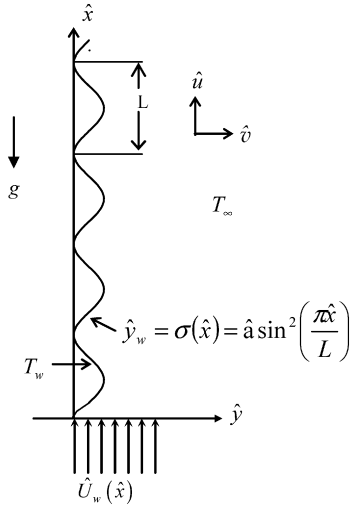

Fig. 1. Physical model and coordinate system.

The boundary conditions for the present problem are

$$\hat{u} = 0, \quad \hat{v} = 0, \quad T = T_w \quad \text{at } \hat{y} = \hat{y}_w = \hat{\sigma}(\hat{x}) \tag{6a}$$

$$\hat{u} = \hat{U}_w(\hat{x}), \quad T = T_\infty \quad \text{as } \hat{y} \to \infty \tag{6b}$$

where T_w is the surface temperature, T_∞ is the ambient temperature of the fluid and $U_w(x)$ is the x component of the inviscid velocity at the surface $\hat{y}_w = \hat{\sigma}(\hat{x})$.

Here q_r is the radiative heat flux in the $\hat{y}$ direction and has been considered the optically dense radiation limit approximation. Thus radiation heat flux term is simplified by the Rosseland diffusion approximation used by [17–29] and is given by

$$q_r = -\frac{4\sigma^*}{3k(\alpha_r + \sigma_s)}\nabla T^4 \tag{7}$$

where σ^* and α_r, σ_s are the Stefan–Boltzmann constant, the Rosseland mean extinction coefficient and the scattering coefficient respectively. The limitation to the use of diffusion approximation should be recognized. It is valid in the interior of a medium but not is employed near the boundaries and is good only for intensive absorption, that is, for an optically thick boundary layer. It cannot provide a complete description of the physical situation near the boundaries since it does not include any terms for radiation from the boundary surface. However, the boundary surface effects are negligible in the interior of an optically thick region since radiation from the boundaries is attenuated before reaching the interior.

Now introduce the following non-dimensional variables:

$$\begin{aligned}
&x = \frac{\hat{x}}{L}, \qquad y = \frac{\hat{y} - \hat{\sigma}(\hat{x})}{L}Re^{1/2}\\
&u = \frac{\hat{u}}{U_\infty}, \qquad U_w = \frac{\hat{U}_w}{U_\infty}\\
&v = \frac{Re^{1/2}}{U_\infty}(\hat{v} - \sigma_x\hat{u}), \qquad p = \frac{\hat{p}}{\rho U_\infty^2}\\
&\theta = \frac{T - T_\infty}{T_w - T_\infty}, \qquad \sigma = \frac{\hat{\sigma}}{L}\\
&\alpha = \frac{\hat{a}}{L}, \qquad \sigma_x = \frac{d\hat{\sigma}}{d\hat{x}}\\
&Re = \frac{\rho U_\infty L}{\mu}, \qquad Gr = \frac{g\beta(T_w - T_\infty)}{\nu^2}L
\end{aligned} \tag{8}$$

where θ is the dimensionless temperature and μ is the dynamic viscosity of the fluid. The x- and y-coordinates are not orthogonal due to the shape of the heated surface, but a regular rectangular computational grid can be easily fitted in the transformed coordinates. It is also worthwhile to point out that (u, v) are the velocity components parallel to (x, y) which are not parallel to the wavy surface and U_∞ is the reference free stream velocity.

On introducing the above dimensionless dependent and independent variables into Eqs. (2)–(5) the following dimensionless form of the governing equations are obtained at leading order in the Reynolds number, Re:

$$\frac{\partial u}{\partial x} + \frac{\partial v}{\partial y} = 0 \tag{9}$$

$$u\frac{\partial u}{\partial x}+v\frac{\partial u}{\partial y}=-\frac{\partial p}{\partial x}+\sigma_x Re^{1/2}\frac{\partial p}{\partial y}+\left(1+\sigma_x^2\right)\frac{\partial^2 u}{\partial y^2}+\frac{Gr}{Re^2}\theta \tag{10}$$

$$\sigma_x\left(u\frac{\partial u}{\partial x}+v\frac{\partial u}{\partial y}\right)+\sigma_{xx}u^2=-Re^{1/2}\frac{\partial p}{\partial y}+\sigma_x\left(1+\sigma_x^2\right)\frac{\partial^2 u}{\partial y^2} \tag{11}$$

$$u\frac{\partial\theta}{\partial x}+v\frac{\partial\theta}{\partial y}=\frac{1}{Pr}\left(1+\sigma_x^2\right)\frac{\partial}{\partial y}\left[\left\{\frac{4}{3}R_d\left(1+(\theta_w-1)\theta\right)^3\right\}\frac{\partial\theta}{\partial y}\right] \tag{12}$$

In the above equations, Pr is the Prandtl number; R_d is the radiation–conduction and θ_w is the surface heating parameters which are defined respectively as,

$$Pr=\frac{\mu C_p}{k},\qquad R_d=\frac{4\sigma^* T_\infty^3}{k(\alpha_r+\sigma_s)},\qquad \theta_w=\frac{T_w}{T_\infty} \tag{13}$$

The term Gr/Re^2 in Eq. (10) represents the Richardson number Ri. The forced convection dominates at small values of Ri, while natural convection takes over at large values of the same parameter. It can easily be seen that the convection induced by the wavy surface is described by Eqs. (9)–(12). We further notice that Eq. (11) indicates that the pressure gradient along the y-direction is of $O(Re^{-1/2})$, which implies that lowest order pressure gradient along x-direction can be determined from the inviscid flow solution and is given by

$$\frac{\partial P}{\partial x}=-\left[\left(1+\sigma_x^2\right)U_w U_w'+\sigma_x\sigma_{xx}U_w^2\right] \tag{14}$$

On the other hand, Eq. (11) shows that $Re^{-1/2}\partial p/\partial y$ is of $O(1)$ and is determined by the left-hand side of this equation. Thus, the elimination of $\partial p/\partial y$ from Eqs. (10) and (11) leads to

$$u\frac{\partial u}{\partial x}+v\frac{\partial u}{\partial y}=\frac{1}{1+\sigma_x^2}\left[-\frac{\partial P}{\partial x}-\sigma_x\sigma_{xx}u^2+\frac{Gr}{Re^2}\theta\right]+\left(1+\sigma_x^2\right)\frac{\partial^2 u}{\partial y^2} \tag{15}$$

The boundary conditions (6) then take the form:

$$u=0,\qquad v=0,\qquad \theta=1\quad \text{at } y=y_w=\sigma(x) \tag{16a}$$

$$u=U_w(x),\qquad \theta=0\quad \text{as } y\to\infty \tag{16b}$$

Now we are in a position to get the solutions of the set of equations consisting of (9), (12), (15) together with the boundary conditions (16) by using the following numerical methods.

3. Numerical methods

Investigating the present problem the authors have employed two numerical methods, namely, implicit finite difference or Keller box method and straightforward finite difference method, which are individually described below.

3.1. Keller box method (KBM)

Before we employ the implicit finite difference method, we need to reduce the aforementioned equations to a convenient set of equations. To do that, we first, introduce the following transformations over the governing equation:

$$\psi=x^{1/2}U_w^{1/2}f(x,\eta)$$
$$\eta=yU_w^{1/2}x^{-1/2}$$
$$\theta=\theta(x,\eta) \tag{17}$$

where η is the pseudo similarity variable and ψ is the stream-function that satisfies Eq. (9) and is defined by

$$u=\frac{\partial\psi}{\partial y},\qquad v=-\frac{\partial\psi}{\partial x} \tag{18}$$

Introducing the transformations given in Eq. (17) into Eqs. (15) and (12) we have,

$$\left(1+\sigma_x^2\right)f'''+\frac{1}{2}\left(1+x\frac{U_w'}{U_w}\right)ff''-x\left(\frac{\sigma_x\sigma_{xx}}{1+\sigma_x^2}+\frac{U_w'}{U_w}\right)\left(f'^2-1\right)+\frac{Gr}{Re^2}\frac{x}{U_w^2}\frac{1}{1+\sigma_x^2}\theta=x\left(f'\frac{\partial f'}{\partial x}-f''\frac{\partial f}{\partial x}\right) \tag{19}$$

$$\frac{1}{Pr}\left(1+\sigma_x^2\right)\left[\left\{1+\frac{4}{3}R_d\left(1+(\theta_w-1)\theta\right)^3\right\}\theta'\right]'+\frac{1}{2}\left(1+x\frac{U_w'}{U_w}\right)f\theta'=x\left(f'\frac{\partial\theta}{\partial x}-\theta'\frac{\partial f}{\partial x}\right) \tag{20}$$

The corresponding boundary conditions are

$$f(x,0)=f'(x,0)=0,\qquad \theta(x,0)=1$$
$$f'(x,\infty)=1,\qquad \theta(x,\infty)=0 \tag{21}$$

There is $U_w'(x)$ and $U_w(x)$ terms appeared in Eqs. (19) and (20). The inviscid solution obtained here is valid only for small values of the amplitude-wavelength ratio. The potential flow solution $U_w(x)$ for small values of $\alpha(\ll 1)$ is

$$U_w(x)=1+\alpha\left[\frac{1}{\pi}\int_0^\infty\frac{\sigma'(t)}{x-t}\,dt\right]+O\left(\alpha^2\right) \tag{22}$$

Removing the singular point of this integral by the residue theorem gives

$$U_w(x)=1+\alpha\left[-\pi\cos(2\pi x)+\int_0^\infty\frac{\sin(2\pi t)}{x+t}\,dt\right]+O\left(\alpha^2\right) \tag{23}$$

However, once we know the values of the function f and θ and their derivatives, it is important to calculate the values of the, local Nusselt number, Nu from the following relations

$$Nu=\frac{\hat{x}[-(k\hat{n}\cdot\nabla T)+\hat{n}\cdot q_r]_{\hat{y}=0}}{k(T_w-T_\infty)} \tag{24}$$

where $\hat{n}$ is the unit normal to the surface. Using the transformation (17) Nu takes the following form:

$$Nu_x Re_x^{-1/2} = -\sqrt{(1+\sigma_x^2)U_w}\left(1+\frac{4}{3}R_d\theta_w^3\right)\theta'(x,0) \tag{25}$$

The total and averaged rate of heat transfer per unit-wetted surface area can be obtained by integrating Eq. (25)

$$Nu_T Re_x^{-1/2} = \int_0^x \left(\frac{U_w}{x}\right)^{1/2}(1+\sigma_x^2) \times \left(1+\frac{4}{3}R_d\theta_w^3\right)\theta'(x,0)\,dx \tag{26}$$

$$Nu_m Re_x^{-1/2} = \frac{x^{1/2}}{S}\int_0^x \left(\frac{U_w}{x}\right)^{1/2}(1+\sigma_x^2) \times \left(1+\frac{4}{3}R_d\theta_w^3\right)\theta'(x,0)\,dx \tag{27}$$

where

$$S = \int_0^x \sqrt{(1+\sigma_x^2)}\,dx \tag{28}$$

Now we are at the position to employ one of the most efficient and accurate implicit finite difference method (the Keller box method) in solving the nonlinear system of partial differential equations (19)–(20) that govern the flow. To employ this method, the set of Eqs. (19)–(20) is written in terms of a system of first order equations in y, which are then expressed in finite difference form by approximating the functions and their derivatives in terms of the central differences in both coordinate directions. Denoting the mesh points in the (x,η) plane by x_i and η_j, where $i = 1,2,3,\ldots,M$ and $j = 1,2,3,\ldots,N$, central difference approximations are made such that the equations involving x explicitly are centred at $(x_{i-1/2},\eta_{j-1/2})$ and the remainder at $(x_i,\eta_{j-1/2})$, where $\eta_{j-1/2} = (\eta_j+\eta_{j-1})/2$, etc. This results in a set of nonlinear difference equations for the unknowns at x_i in terms of their values at x_{i-1}. These equations are then linearized by the Newton's quasi-linearization technique and are solved using a block-tridiagonal algorithm, taking as the initial iteration of the converged solution at $x = x_{i-1}$. Now to initiate the process at $x = 0$, we first provide guess profiles for all five variables (arising the reduction to the first order form) and use the Keller box method to solve the governing ordinary differential equations. Having obtained the lower stagnation point solution it is possible to march step by step along the boundary layer. For a given value of x, the iterative procedure is stopped when the difference in computing the velocity and the temperature in the next iteration is less than 10^{-5}, i.e. when $|\delta f^i| \leqslant 10^{-5}$, where the superscript denotes the iteration number. The computations were not performed using a uniform grid in the y direction, but a non-uniform grid was used and defined by $\eta_j = \sinh((j-1)/p)$, with $j = 1,2,\ldots,301$ and $p = 100$.

3.2. Straightforward finite difference method (SFFD)

As before, we reduce the set of Eqs. (9), (15) and (12) to a convenient form for employing the straight-forward finite difference method by introducing a new group of transformations as given in (29)

$$X = x, \qquad Y = y\left(\frac{x}{U_w}\right)^{-1/2}$$
$$U = \frac{u}{U_w}, \qquad V = v\left(\frac{x}{U_w}\right)^{1/2} \tag{29}$$

Using (29) into (9), (15) and (12), we get

$$X\frac{\partial U}{\partial X} - \frac{1}{2}Y\left(1-X\frac{U_w'}{U_w}\right)\frac{\partial U}{\partial X} + \frac{\partial V}{\partial Y} + X\frac{U_w'}{U_w}U = 0 \tag{30}$$

$$XU\frac{\partial U}{\partial X} + \left[V - \frac{1}{2}UY\left(1-X\frac{U_w'}{U_w}\right)\right]\frac{\partial U}{\partial Y} + X\left(\frac{U_w'}{U_w} + \frac{\sigma_x\sigma_{xx}}{1+\sigma_x^2}\right)(U^2-1) = (1+\sigma_x^2)\frac{\partial^2 u}{\partial Y^2} + \frac{1}{1+\sigma_x^2}\frac{Gr}{Re^2}\frac{X}{U_w^2}\theta \tag{31}$$

$$XU\frac{\partial\theta}{\partial X} + \left[V - \frac{1}{2}UY\left(1-X\frac{U_w'}{U_w}\right)\right]\frac{\partial\theta}{\partial Y} = \frac{1}{Pr}(1+\sigma_x^2)\frac{\partial}{\partial Y}\left[\left\{1+\frac{4}{3}R_d\left(1+(\theta_w-1)\theta\right)^3\right\}\frac{\partial\theta}{\partial Y}\right] \tag{32}$$

The corresponding boundary conditions are

(1) On the wavy surface ($Y = 0$):

$$U = V = 0, \qquad \theta = 1 \tag{33a}$$

(2) Matching with the inviscid flow ($Y \to \infty$)

$$U \to 1, \qquad \theta \to 0 \tag{33b}$$

Now Eqs. (30)–(32) subject to the boundary conditions (33) are discretized for straightforward finite difference (SFFD) method using central-difference for diffusion terms and the forward-difference for the convection terms, finally we get a system of tri-diagonal algebraic equations which are solved by Gaussian elimination technique. The computation is started at $X = 0.0$, and then marches downstream implicitly. Here we have taken $\Delta X = 0.005$ and $\Delta Y = 0.01$ for the X- and Y-grids respectively. We are at the position to measure of the physical quantities, namely the local, total and the average rate of heat transfer which are important from the application point of view, from the following dimensionless relations:

$$Nu_x Re_x^{-1/2} = -\sqrt{(1+\sigma_x^2)U_w}\left(1+\frac{4}{3}R_d\theta_w^3\right)\left(\frac{\partial\theta}{\partial Y}\right)_{Y=0} \tag{34}$$

$$Nu_T Re_x^{-1/2} = \int_0^X \left(\frac{U_w}{X}\right)^{1/2}(1+\sigma_x^2) \times \left(1+\frac{4}{3}R_d\theta_w^3\right)\left(\frac{\partial\theta}{\partial Y}\right)_{Y=0} dX \tag{35}$$

$$Nu_m Re_x^{-1/2} = \frac{X^{1/2}}{S}\int_0^X \left(\frac{U_w}{X}\right)^{1/2}\left(1+\sigma_x^2\right) \times \left(1+\frac{4}{3}R_d\theta_w^3\right)\left(\frac{\partial\theta}{\partial Y}\right)_{Y=0} dX \quad (36)$$

4. Results and discussion

The governing equations (19)–(21) are solved by very efficient Keller-box method (KBM) and the straightforward finite difference method (SFFD) is used to solve Eqs. (30)–(33). The numerical results are presented by Figs. 2–10 using KBM and the SFFD results are shown in Figs. 3(b) and 4(b) for comparing with Keller box (KBM) results. The numerical results for the rate of heat transfer in terms of the local Nusselt number $Nu_x Re_x^{-1/2}$ and the average rate of heat transfer $Nu_m Re_x^{-1/2}$ and the total rate of heat transfer $Nu_T Re_x^{-1/2}$ are obtained for representative values of the Planck number $R_d(= 0.0, 0.5, 1.0)$, surface heating parameter $\theta_w(= 1.1, 1.3, 1.5)$, amplitude of the wavy surface $\alpha(= 0.0, 0.05, 0.1, 0.2)$ and the mixed convection parameter or the Richardson number $Ri(= 1.0, 5.0, 10.0)$. It should be noted that for CO_2 in the temperature range of 100–650 F (with the corresponding Prandtl number range 0.76–0.6) and NH_3 vapour in the temperature range of 120–400 F (with the corresponding Prandtl number 0.88–0.84) at 1 atm. the value of R_d ranges from 0.033 to 0.1, whereas water vapour in the temperature range of 220–900 F (with the corresponding Prandtl number $Pr \approx 1.0$) the R_d values lie between 0.02 and 0.3 (see Cess [18]).

Fig. 2 depicts the comparisons of the present numerical results of the inviscid velocity as well as the local Nusselt number with the results obtained by Cheng and Wang [8]. Here, the interaction of the Planck number R_d is ignored and Richardson number $Ri = 0.0$ are chosen. The present results by Keller box method (KBM) agreed well with the solutions of Cheng and Wang [8] in the absence of micropolar parameter.

The numerical results of the local Nusselt number $Nu_x Re_x^{-1/2}$ and the average rate of heat transfer $Nu_m Re_x^{-1/2}$ for different values of the Planck number $R_d(= 0.0, 0.5, 1.0)$ while $\theta_w = 1.1, \alpha = 0.05$ and $Pr = 1.0$ are illustrated in Figs. 3(a)–(b) respectively. From the Fig. 3(b), it should be noticed that the agreement between the results obtained by using the Keller box method (KBM) and the straightforward finite difference method (SFFD) is very good indeed. From the figures, it can be seen that an increase in the Planck number R_d leads to an increase the local Nusselt number $Nu_x Re_x^{-1/2}$ and the average rate of heat transfer $Nu_m Re_x^{-1/2}$. This may be attributed to the fact that the increase of the values of R_d implies more interaction of radiation with the thermal boundary layers and consequently the heat absorption intensity of the fluid increases. For a complete cycle ($1 < x < 2$), the maximum value is located at 1.36, not at the crest ($x = 1.5$) of the wavy surface, and the minimum value is located at the leading edge. The important fact is that the average rate of heat transfer is larger than the local Nusselt number.

The effect of the surface heating parameter $\theta_w(= 1.1, 1.3, 1.5)$ on the local Nusselt number $Nu_x Re_x^{-1/2}$ and the average rate of heat transfer $Nu_m Re_x^{-1/2}$ are shown in Fig. 4(a)–(b) respectively while $R_d = 1.0$, $\alpha = 0.05$ and $Pr = 1.0$. We notice that an increase in the values of the surface heating parameter θ_w leads to enhance in the results of $Nu_x Re_x^{-1/2}$ and $Nu_m Re_x^{-1/2}$. This phenomenon can easily be understood from the fact that when the surface heating parameter θ_w increases, the temperature of the surface rises. For balancing the temperature difference between surface and fluid the local Nusselt number $Nu_x Re_x^{-1/2}$ and the corresponding average rate of heat transfer $Nu_m Re_x^{-1/2}$ increase.

Fig. 5(a)–(b) show the effect of the Richardson number $Ri(= 1.0, 5.0, 10.0)$ on the local rate of heat transfer $Nu_x Re_x^{-1/2}$ and the total rate of heat transfer $Nu_T Re_x^{-1/2}$. For $Ri(= 1)$ the flow induces by mixed convection and for large $Ri(> 1)$ the flow induces by natural convection. It is clearly seen that for mixed convection the local and total rate of heat transfer always smaller than that of the natural convection. The effect of the surface waviness $\alpha(= 0.0, 0.05, 0.1, 0.2)$ on the local and total rate of heat transfer has been illustrated in Fig. 6(a)–(b). The local and total rate of heat transfer takes wavy form for the surface waviness. For large values of α, the local rate of heat transfer decreases slowly, but the total heat transfer rate for the wavy surface is indeed greater than that of a flat plate. It seems to convey and incorrect impression that a wavy surface is inferior in enhancing mixed convection heat transfer. The total heat transfer is a more important factor in designing a heat-transfer device than its local rate.

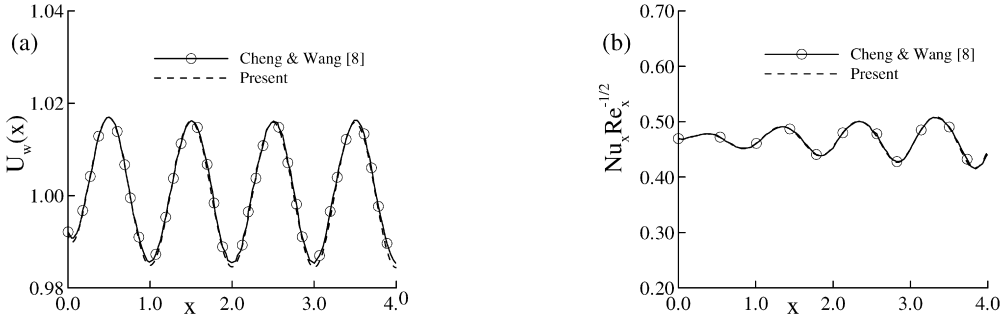

Fig. 2. Comparison of the present results with the results of Chang and Wang [8]. (a) Inviscid velocity for $\alpha = 0.005$. (b) Local Nusselt number for $Pr = 1.0$, $\alpha = 0.002$, $R_d = 0.0$ and $Ri = 0.0$.

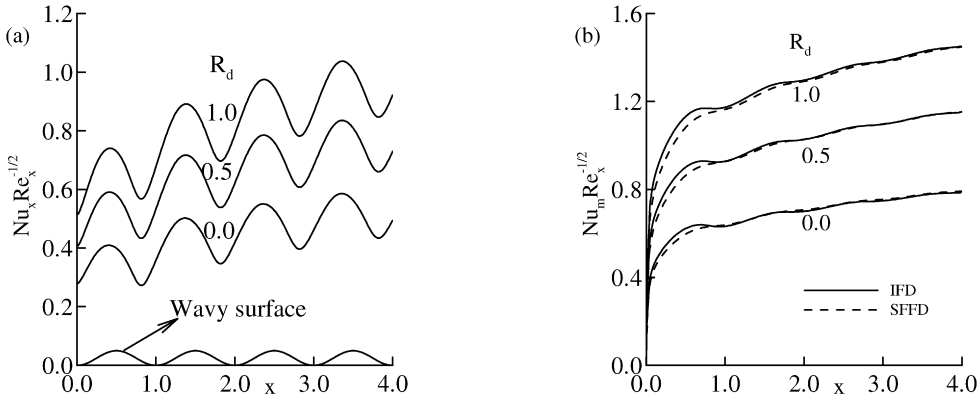

Fig. 3. (a) Local Nusselt number. (b) Average Nusselt number for different values R_d of while $Pr = 0.7$, $\alpha = 0.05$, $\theta_w = 1.1$ and $Ri = 1.0$.

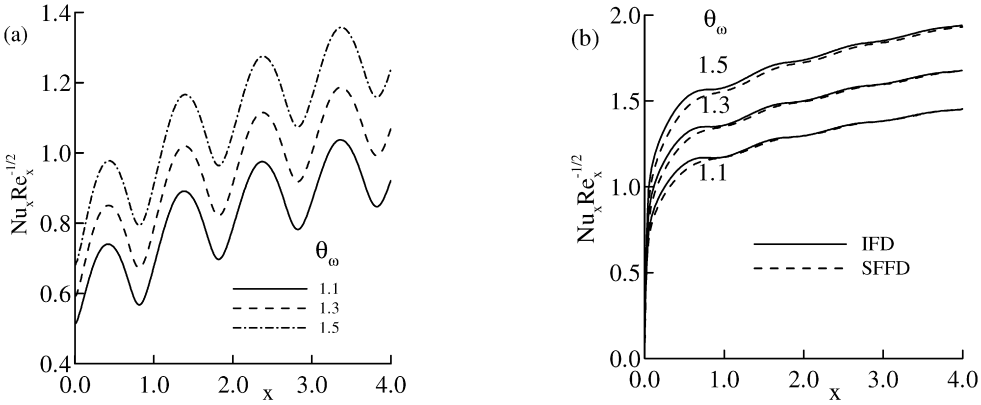

Fig. 4. (a) Local Nusselt number. (b) Average Nusselt number for different values of θ_w while $Pr = 0.7$, $\alpha = 0.05$, $R_d = 1.0$ and $Ri = 1.0$.

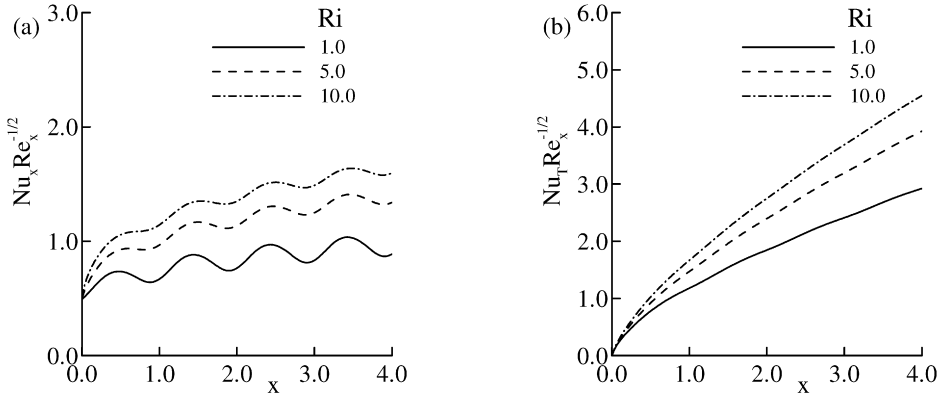

Fig. 5. (a) Local Nusselt number. (b) Total Nusselt number for different values of Ri while $Pr = 0.7$, $R_d = 1.0$, $\theta_w = 1.1$ and $\alpha = 0.05$.

Attention is now given to the effects of pertinent parameters on the dimensionless velocity and temperature in the flow field. Figs. 5 and 6 illustrate the velocity and temperature distributions against η for different values of the Planck number and the surface heating parameter θ_w. These figures display how R_d and θ_w influence on the fluid velocity and temperature. In Fig. 7(a)–(b), the effects of the Planck number R_d on the fluid velocity and temperature are shown. The choice of Planck number has also a substantial effect on the velocity and temperature distributions in the boundary layer. When R_d increases, the fluid velocity and the temperature increases. The reason of this practical scenario is that the R_d leads to raise the velocity gradients which accelerate the fluid motion and the corresponding temperature distribution increases due to enhanced heat absorption intensity of the fluid. It is seen that at the crest, the temperature distribution is larger than the trough temperature which is expected. In Fig. 8(a)–(b), as θ_w increases, the velocity and temperature gradients at the surface increase which again enhance the fluid velocity and temperature. The local maximum velocities for the crest are obtained for $\theta_w = 1.1$, 1.3 and 1.5, which are 1.17633, 1.22256 and 1.27285 at $\eta = 2.70, 2.59$ and 2.48 respectively. The maximum velocity of the fluid increase by 8.20% as θ_w increases from 1.1 to 1.5. Also the temperature

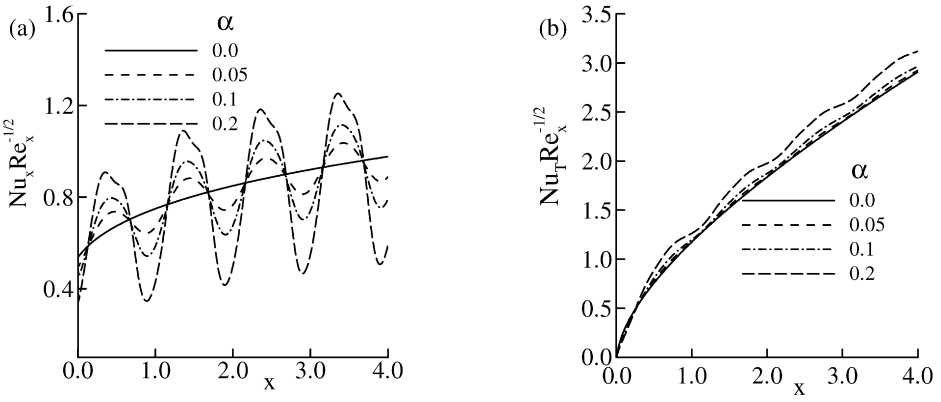

Fig. 6. (a) Local Nusselt number. (b) Total Nusselt number for different values of α while $Pr = 0.7$, $R_d = 1.0$, $\theta_w = 1.1$ and $Ri = 1.0$.

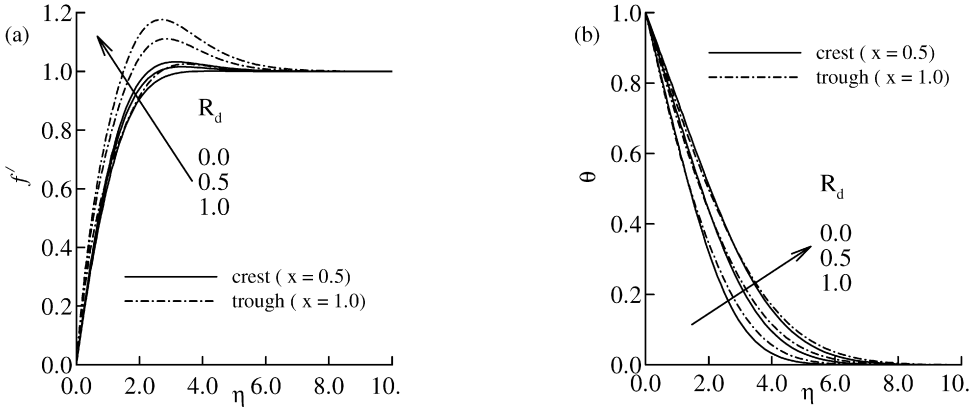

Fig. 7. (a) Velocity. (b) Temperature distribution for different values of R_d while $Pr = 0.7$, $\alpha = 0.05$, $Ri = 1.0$ and $\theta_w = 1.1$ at crest ($x = 0.5$) and trough ($x = 1.0$).

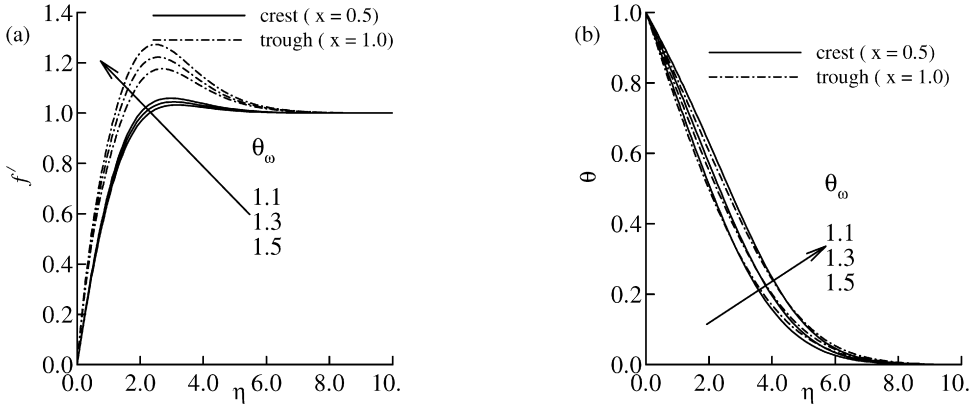

Fig. 8. (a) Velocity. (b) Temperature distribution for different values of θ_w while $Pr = 0.7$, $\alpha = 0.05$, $Ri = 1.0$ and $R_d = 1.0$ at crest ($x = 0.5$) and trough ($x = 1.0$).

increases by 30.19% at $\eta = 2.70$. Finally, it is conclude that the maximum velocity occur at the trough no at the crest.

Figs. 9 and 10 illustrate the effect of the radiation–conduction parameter R_d on the development of streamlines and isotherms respectively, which are plotted for $\alpha = 0.05$, $Pr = 1.0$, $Ri = 1.0$ and $\theta_w = 1.1$. It is seen that without effect of radiation (i.e. $R_d = 0.0$) the value of $\psi_{\max}$ within the computational domain is 19.68. From Fig. 9(b) for $R_d = 1.0$ the value of $\psi_{\max}$ is 20.84. It can be concluded that with the effect of the radiation–conduction parameter R_d, the flow flux in the boundary layer increases due to increase the driving force that means buoyancy force. From Fig. 10(a)–(b), it can be seen that with the effect of R_d the thermal boundary layer thickness increases significantly. Due to the effect of radiation, the temperature gradient increase (see Fig. 3(a)) and hence the temperature distribution enhances within the boundary layer.

5. Conclusion

The effect of radiation on mixed convection flow along an isothermal vertical wavy surface has been investigated numerically. The governing boundary layer equations of mo-

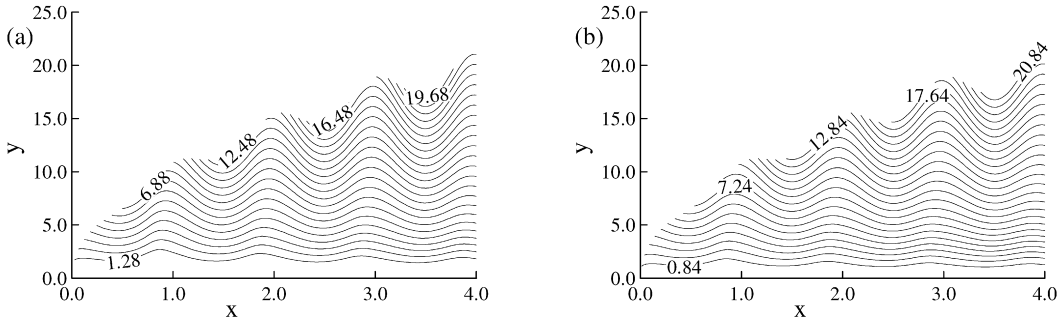

Fig. 9. Streamlines for (a) $R_d = 0.0$ (b) $R_d = 1.0$ while $Pr = 0.7$, $\alpha = 0.05$, $Ri = 1.0$ and $\theta_w = 1.1$, where $\Delta\psi = 0.8$.

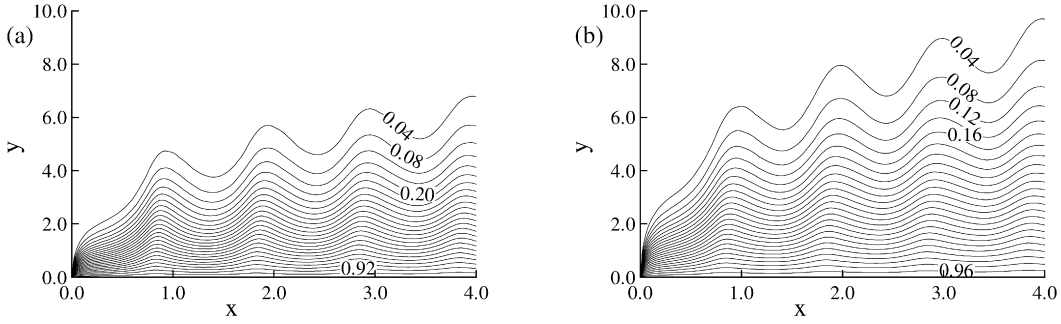

Fig. 10. Isotherms for (a) $R_d = 0.0$ (b) $R_d = 1.0$ while $Pr = 0.7$, $\alpha = 0.05$, $Ri = 1.0$ and $\theta_w = 1.1$, where $\Delta\theta = 0.04$.

tion are transformed into a non-dimensional form and the resulting nonlinear systems of partial differential equations are solved numerically by two distinct efficient methods namely (i) Implicit finite difference method together with Keller-box scheme (KBM) and (ii) Straightforward finite difference method (SFFD). From the present investigation the following conclusions may be drawn:

- The local Nusselt number $Nu_x Re_x^{-1/2}$ and the average rate of heat transfer $Nu_m Re_x^{-1/2}$ increase when the value of the radiation–conduction parameter R_d and surface heating parameter θ_w increase.
- As R_d and θ_w increase, both the velocity and the temperature distribution increase significantly at trough of the wavy surface.
- For increasing values of R_d, the momentum and thermal boundary layer thickness enhanced.
- For large values of Ri, the local and total rate of heat transfer enhanced.
- The total rate of heat transfer increases as the surface roughness increases.

References

[1] L.S. Yao, Natural convection along a vertical complex wavy surface, Int. J. Heat Mass Transfer 49 (2006) 281–286.

[2] L.S. Yao, Natural convection along a vertical wavy surface, ASME J. Heat Transfer 105 (1983) 465–468.

[3] S.G. Moulic, L.S. Yao, Natural convection along a wavy surface with uniform heat flux, ASME J. Heat Transfer 111 (1989) 1106–1108.

[4] S.G. Moulic, L.S. Yao, Mixed convection along wavy surface, ASME J. Heat Transfer 111 (1989) 974–979.

[5] M.A. Hossain, I. Pop, Magnetohydrodynamic boundary layer flow and heat transfer on a continuous moving wavy surface, Arch. Mech. 48 (1996) 813–823.

[6] K.C.A. Alam, M.A. Hossain, D.A.S. Rees, Magnetohydrodynamic free convection along a vertical wavy surface, Appl. Mech. Engrg. 1 (1997) 555–566.

[7] I. Pop, T.Y. Na, Natural convection over a vertical wavy frustum of a cone, Int. J. Non-Linear Mech. 34 (1999) 925–934.

[8] C.W. Cheng, C.C. Wang, Forced convection in micropolar fluid over a wavy surface, Numer. Heat Transfer, Part A 37 (2000) 271–287.

[9] M.A. Hossain, D.A.S. Rees, Combined heat and mass transfer in natural convection flow from a vertical wavy surface, Acta Mech. 136 (1999) 133–141.

[10] M.A. Hossain, M.S. Munir, I. Pop, Natural convection flow of viscous fluid with viscosity inversely proportional to linear function of temperature from a vertical cone, Int. J. Therm. Sci. 40 (2001) 366–371.

[11] M.A. Hossain, S. Kabir, D.A.S. Rees, Natural convection of fluid with temperature dependent viscosity from heated vertical wavy surface, ZAMP 53 (2002) 48–52.

[12] M.M. Molla, M.A. Hossain, L.S. Yao, Natural convection flow along a vertical wavy surface with uniform surface temperature in presence of heat generation/absorption, Int. J. Therm. Sci. 43 (2004) 157–163.

[13] J.H. Jang, W.M. Yan, H.C. Liu, Natural convection heat and mass transfer along a vertical wavy surface, Int. J. Heat Mass Transfer 46 (2003) 1075–1083.

[14] J.H. Jang, W.M. Yan, Mixed convection heat and mass transfer along a vertical wavy surface, Int. J. Heat Mass Transfer 47 (2004) 419–428.

[15] J.H. Jang, W.M. Yan, Transient analysis of heat and mass transfer by natural convection over a vertical wavy surface, Int. J. Heat Mass Transfer 47 (2004) 3695–3705.

[16] S. Rosseland, Theoretical Astrophysics, Oxford University Press, London, 1936.

[17] R. Goulard, M. Goulard, Energy transfer in the Couette flow of a radiation and chemically reacting gas, in: Proceeding of the Heat Transfer and Fluid Mechanics Institute, Stanford University Press, Palo Alto, CA, 1959, pp. 126–139.

[18] R.D. Cess, The interaction of thermal radiation with free convection heat transfer, Int. J. Heat Mass Transfer 9 (1966) 1269–1277.

[19] V.S. Arpaci, Effect of thermal radiation on the laminar free convection from a heated vertical plate, Int. J. Heat Mass Transfer 11 (1968) 871–881.
[20] E.H. Cheng, M.N. Ozisic, Radiation with free convection in an absorbing, emitting and scattering medium, Int. J. Heat Mass Transfer 15 (1972) 1243–1252.
[21] J. Shwartz, Radiation coupled viscous flows, Int. J. Heat Mass Transfer 11 (1968) 689–697.
[22] M.A. Hossain, H.S. Takhar, Radiation effect on mixed convection along a vertical plate with uniform surface temperature, Heat Mass Transfer 31 (1996) 243–248.
[23] M.A. Hossain, D.A.S. Rees, I. Pop, Free convection–radiation interaction from an isothermal plate inclined at a small angle to the horizontal, Acta Mech. 127 (1998) 63–73.
[24] M.A. Hossain, M.A. Alim, D.A.S. Rees, The effect of radiation on free convection from a porous vertical plate, Int. J. Heat Mass Transfer 42 (1999) 181–191.
[25] M.A. Hossain, M.A. Alim, D.A.S. Rees, Effect of thermal radiation on natural convection over cylinders of elliptic cross section, Acta Mech. 129 (1998) 177–186.
[26] M.A. Hossain, M.A. Alim, Natural convection–radiation interaction on boundary layer flow along a thin vertical cylinder, Heat Mass Transfer 32 (1997) 515–520.
[27] M.A. Hossain, M. Kutubuddin, I. Pop, Radiation–conduction interaction on mixed convection from a horizontal circular cylinder, Heat Mass Transfer 35 (1999) 307–314.
[28] K.A. Yih, Effect of radiation on natural convection about a truncated cone, Int. J. Heat Mass Transfer 42 (1999) 4299–4305.
[29] M.M. Molla, M.A. Hossain, M.C. Paul, Radiation effect on natural convection flow from an isothermal sphere, Int. J. Fluid Mech. Res., in press.
[30] T. Cebeci, P. Bradshaw, Physical and Computational Aspects of Convective Heat Transfer, Springer, New York, 1984.
[31] H.B. Keller, Numerical methods in boundary layer theory, Annual Rev. Fluid Mech. 10 (1978) 417–433.